FEBS Open Bio 5 (2015) 605–614

journal homepage: www.elsevier.com/locate/febsopenbio

Proteasome inhibitors prevent cell death and prolong survival of mice challenged by Shiga toxin

Takayuki Hattori [a], Miho Watanabe-Takahashi [b], Nobumichi Ohoka [a], Takashi Hamabata [c], Koichi Furukawa [d], Kiyotaka Nishikawa [b], Mikihiko Naito [a,*]

[a] Division of Molecular Target and Gene Therapy Products, National Institute of Health Sciences, Tokyo 158-8501, Japan
[b] Faculty of Life and Medical Sciences, Doshisha University, Kyoto 610-0394, Japan
[c] Research Institute, National Center for Global Health and Medicine, Tokyo 162-8655, Japan
[d] Department of Biochemistry II, Nagoya University Graduate School of Medicine, Nagoya 466-0065, Japan

ARTICLE INFO

Article history:
Received 30 April 2015
Revised 5 June 2015
Accepted 8 June 2015

Keywords:
Shiga toxin
Apoptosis
Apoptosis inhibitory proteins
Proteasome
Proteasome inhibitor

ABSTRACT

Shiga toxin (Stx) causes fatal systemic complications. Stx induces apoptosis, but the mechanism of which is unclear. We report that Stx induced rapid reduction of short-lived anti-apoptotic proteins followed by activation of caspase 9 and the progression of apoptosis. Proteasome inhibitors prevented the reduction of anti-apoptotic proteins, and inhibited caspase activation and apoptosis, suggesting that the reduction of anti-apoptotic proteins is a prerequisite for Stx-induced apoptosis. A clinically approved proteasome inhibitor, bortezomib, prolonged the survival of mice challenged by Stx. These results imply that proteasome inhibition may be a novel approach to prevent the fatal effects of Stx.

1. Introduction

Stx-producing *Escherichia coli* (STEC), including O157, O104 and O111, causes diarrhea and hemorrhagic colitis in the gut. When Stx traverses the epithelium and passes into the circulation system, it occasionally causes systemic complications such as encephalopathy and hemolytic-uremic syndrome sometimes resulting in the death of the infected patients [1–4]. Therefore, the development of an antidote to prevent the lethal effects of Stx is urgently required.

Stx can be classified into two groups, Stx type 1 (Stx1) and type 2 (Stx2) [5,6], with Stx2 linked to severer diseases epidemiologically. The Stx holotoxin is composed of one molecule of the A-subunit that has RNA *N*-glycosidase activity and five molecules of the B-subunit. The pentameric B-subunit facilitates the binding of Stx to the cell surface receptors, globotriaosylceramide (Gal α(1-4)-Galβ(1-4)-Glcβ-ceramide (Gb3)/CD77) [6,7]. After internalization, Stx is transported from the early endosomes to the ER via the Golgi apparatus. Stx then catalyzes the removal of adenine at position 4324 of 28S rRNA, thereby inhibiting protein biosynthesis [8,9].

Several studies indicated that Stx induces apoptosis in some cells, implying that induction of apoptosis is, at least in part, crucial for vascular lesions and tissue damage after translocation of Stx into the circulation system [10]. These studies include Stx inducing rapid apoptotic cell death in several CD77-positive cell lines such as myelogenous leukemia cell line THP1, epithelial cell lines and Burkitt's lymphoma cell lines [11–14] in a mitochondrial pathway-dependent manner. In other studies, however, it was reported that Stx induces apoptosis through ER stress responses, including the activation of IRE1, PERK and ATF6, and an increase in the expression level of CHOP in THP1 cells [15,16]. In these reports, Stx treatment increased the expression of a death ligand, TRAIL and its cell surface receptor, DR5 which mediates activation of caspase 8. Garibal et al. reported that caspase 8-mediated cleavage of Bid is required for Stx1-induced apoptosis in Burkitt's lymphoma cells [17]. Induction of apoptosis by Stx through the activation of caspase 8, 6 and 3, but not the caspase 9-dependent mitochondrial pathway was also reported in HeLa cells [18].

Abbreviations: Stx, Shiga toxin; STEC, Shiga toxin-producing *Escherichia coli*; ER, endoplasmic reticulum; FLIP, FLICE (FADD-like IL-1β-converting enzyme)-inhibitory protein; c-IAP1, cellular inhibitor of apoptosis protein 1; Mcl-1, myeloid cell leukemia 1; PARP, Poly(ADP-ribose) polymerase; PI, propidium iodide; BRZ, bortezomib; CHX, cycloheximide

* Corresponding author at: Division of Molecular Target and Gene Therapy Products, National Institute of Health Sciences, Kamiyoga 1-18-1, Setagaya-ku, Tokyo 158-8501, Japan. Tel.: +81 3 3700 9428; fax: +81 3 3707 6950.
E-mail address: miki-naito@nihs.go.jp (M. Naito).

http://dx.doi.org/10.1016/j.fob.2015.06.005

Thus, the cell death mechanism induced by Stx is complicated, and it is unclear whether the inhibition of apoptosis could be beneficial for preventing the fatal effects of Stx.

In this study, we investigated the cell death mechanism in THP1 cells and CD77 synthase transfected U937 cells. We found that the Stx induced apoptosis in CD77-expressing cells in a caspase-dependent manner with caspase 9 as the primary initiator caspase. Upon Stx treatment, apoptosis inhibitory proteins were rapidly downregulated, and proteasome inhibitors prevented the reduction of them and the progression of apoptosis. We also demonstrate that clinically approved proteasome inhibitor, bortezomib [19] suppressed Stx-induced apoptosis and prolonged the survival of mice challenged by a lethal dose of Stx.

2. Materials and methods

2.1. Reagents

RPMI1640, tunicamycin, PI, anti-α-tubulin antibody (B-5-1-2), anti-β-actin antibody (AC-74) and anti-FLAG antibody (M2) were purchased from Sigma. Z-VAD-fmk and MG132 were from the Peptide Institute. Etoposide was obtained from Bristol-Myers Squibb. Bortezomib was from LC Laboratories. The anti-Hsp90 antibody (68), anti-Mcl-1 antibody (22), anti-Bcl-x antibody and anti-Bcl-2 antibody (7) were from BD Biosciences. The anti-PARP antibody (46D11) and anti-β-catenin antibody were from Cell Signaling Technology. The anti-caspase 3 antibody (H-277), anti-CHOP antibody (R-20), anti-GAPDH antibody (FL-335) and anti-caspase 9 antibody (H-17) were from Santa Cruz. The anti-XIAP antibody, anti-caspase 8 antibody (5F7), anti-caspase 9 antibody (5B4) and anti-caspase 10 antibody (4C1) were from Medical & Biological Laboratories. The anti-c-IAP1 antibody was from R&D Systems. The anti-FLIP antibody and anti-Apaf1 antibody were from Enzo. The anti-Apollon antibody [20], recombinant Stx1 and Stx2 [21] and Stx1 A-subunit mutant (E167Q/R170L) [22] were prepared as described previously.

2.2. Cell culture

THP1 cells and U937 cells were purchased from the American Type Culture Collection and cultured in RPMI1640 containing 10% fetal bovine serum and antibiotics. Cells were grown in 5% CO_2 at 37 °C in a humidified atmosphere.

2.3. Measurement of the incorporation of PI

Cells were resuspended in staining buffer (SB, 3% calf serum in PBS (−)) containing 2 μg/ml PI. Fluorescence and phase contrast images were obtained by BIOREVO (Keyence). PI-positive cells were counted with FACSCalibur (BD Biosciences).

2.4. Mammalian expression vector for CD77 synthase and isolation of transformants

Human CD77 synthase cDNA [23,24] was amplified by polymerase chain reaction and inserted into the p3 × FLAG-CMV10 vector (Sigma). U937 cells were pulsed with a Gene Pulser II Electroporation System (BIO-RAD) at 250 V and 950 μF in the presence of 50 μg of the expression vector. After recovery for 48 h, the cells were selected with 1 mg/ml G418.

2.5. Measurement of cell surface CD77

CD77 synthase-transfected U937 cell clones were resuspended in SB containing fluorescein isothiocyanate (FITC)-conjugated anti-CD77 antibody (5B5, BD Biosciences) and incubated on ice for 20 min. The cells were then washed with SB twice and the expression of CD77 was measured with FACSCalibur.

2.6. Pull-down of initially activated caspases with biotinylated Z-VAD-fmk

Initially activated caspase was detected according to the previous report [25]. Briefly, 10^7 cells in 1 ml of culture media were pre-incubated with 50 μM biotinyl-VAD-fmk (MP Biomedicals) for 1 h, and then treated with the indicated apoptosis inducers. Following stimulation, cells were harvested and lysed in KCl lysis buffer (50 mM HEPES (pH 7.4), 142.5 mM KCl, 5 mM $MgCl_2$, 1 mM EGTA, 1% NP-40 and protease inhibitors). After centrifugation at >15,000*g* at 4 °C for 15 min, streptavidin-agarose was added to the supernatants and incubated at 4 °C overnight. Then, the agarose was washed four times with the KCl lysis buffer. Precipitated caspases were analyzed by Western blotting.

2.7. Immunoprecipitation (IP) and immunoblotting

After treatment, cell lysates were prepared with IP buffer (50 mM Tris-HCl (pH 7.5), 150 mM NaCl and 0.5% Triton-X 100) supplemented with protease inhibitors and analyzed by immunoprecipitation and immunoblotting as described previously [26].

2.8. Animal experiments

All animal experiments were approved by the animal ethics committee of Doshisha University according to the guidelines for animal experimentation of the Ministry of Education, Culture, Sports, Science and Technology, Japan. Pathogen-free female ICR mice were purchased from Japan SLC. Mice were housed under a 12 h light-dark cycle and fed a standard diet. Mice were injected intravenously with 0.1 ml of sterile saline solution supplemented with mannitol alone or with various doses of bortezomib prior to administration of a lethal dose of Stx2 (0.15 ng/g of body weight) as described in the legend to Fig. 6, and monitored at the indicated times.

2.9. Statistical analysis

For analysis of cell viability, PI positive cells were analyzed by unpaired two tailed Student's *t*-test.

3. Results

3.1. Stx induces apoptosis in a caspase-dependent manner

To gain insights into the mechanism of Stx-induced apoptosis, we first searched for cell lines that undergo rapid apoptosis upon Stx treatment. Among the 25 cell lines tested, THP1 showed the highest sensitivity to Stx-induced apoptosis (Table 1). Fig. 1A shows that Stx induced apoptosis-like morphological changes in THP1 cells as reported previously [27]. Cell death was confirmed by PI-staining and approximately 80% of the treated cells were PI-positive after 24 h. Both Stx1 and Stx2 induced caspase 3 activation and Poly(ADP-ribose) polymerase (PARP) cleavage 4 h after treatment (Fig. 1B). In our experiments, Stx did not induce the expression of CHOP, a marker of ER stress response [28] within 8 h following Stx treatment, whereas the glycosylation inhibitor tunicamycin induced CHOP expression 6 h after treatment, indicating that the ER stress response is not involved in the Stx-induced apoptosis under this condition. Stx1 (Fig. 1C) and Stx2 (Fig. 1D) induced caspase activation in a dose-dependent manner. The

Table 1
Induction of apoptosis by Stx in the 25 cell lines we tested[a].

Cell line	Induction of apoptosis by Stx	Tissue	Morphology	Organism
THP1	+++	Peripheral blood	Monocyte	*H. sapiens*
U937	–	Pleural effusion, lymphocyte, myeloid	Monocyte	*H. sapiens*
Raji	+	Lymphoblast	Lymphoblast	*H. sapiens*
K562	–	Bone marrow	Lymphoblast	*H. sapiens*
HL60	–	Peripheral blood	Myeloblastic	*H. sapiens*
KYO-1	–	Peripheral blood	Myeloblastic	*H. sapiens*
CCRF-CEM	–	Peripheral blood	Lymphoblast	*H. sapiens*
Jurkat	–	Peripheral blood	Lymphoblast	*H. sapiens*
HEL	–	Bone marrow	Lymphoblast	*H. sapiens*
MOLT4	–	T lymphoblast	Lymphoblast	*H. sapiens*
A549	–	Lung	Epithelial	*H. sapiens*
HeLa	–	Cervix	Epithelial	*H. sapiens*
HEK-293	–	Embryonic kidney	Epithelial	*H. sapiens*
Caco-2	–	Colon	Epithelial-like	*H. sapiens*
U-2 OS	–	Bone	Epithelial	*H. sapiens*
HT1080	–	Connective tissue	Epithelial	*H. sapiens*
MBEC2, 4, 6, 7	–	Brain	Endothelial	*M. musculus*
M1	–	Bone marrow	Myeloblast	*M. musculus*
SP2/0	–	Spleen	Lymphoblast-like	*M. musculus*
P388	–	Monocyte, macrophage	Lymphoblast	*M. musculus*
Vero	+	Kidney	Epithelial	*C. aethiops*
COS-1	–	Kidney	Fibroblast	*C. aethiops*

[a] Cells were treated with either 400 ng/ml Stx1 or Stx2 for up to 48 h, and apoptotic morphological changes were monitored.

threshold values of caspase activation were 1 pg/ml for Stx1 and 0.01 pg/ml for Stx2, which is consistent with the observation that Stx2 is more toxic than Stx1 both *in vitro* and *in vivo* [29]. To examine the role of caspase in Stx-induced apoptosis, we treated the THP1 cells with the pan-caspase inhibitor Z-VAD-fmk prior to the Stx treatment. Stx-induced apoptosis was markedly suppressed by Z-VAD-fmk (Fig. 1A). These observations indicate that Stx induces apoptosis in a caspase-dependent manner.

During the onset of apoptosis, an executioner caspase (caspase 3) is activated by an initiator caspase, such as caspases 8, 9 and 10. Caspase 8/10 is normally activated by death receptor ligation, whereas caspase 9 is activated via a mitochondrial pathway. Therefore, we next tried to identify the initiator caspase activated by Stx treatment by *in situ* trapping of the activated caspases [25]. THP1 cells were pre-incubated with biotinyl-VAD-fmk and then treated with Stx1 or a DNA-damaging agent etoposide to initiate caspase activation so that the activated caspases are covalently labeled with biotinyl-VAD-fmk. After cell lysis, the biotinylated proteins were precipitated with streptavidin agarose and the precipitates were analyzed by Western blotting. As shown in Fig. 2A, when cells were treated with Stx1, an active caspase 9 fragment was biotinylated; however, caspases 8 and 10 were not biotinylated. The caspase 9 fragment was also labeled with biotinyl-VAD-fmk in etoposide-treated cells, whereas none of the caspases were biotinylated in the control cells.

Since THP1 cells did not undergo apoptosis by death receptor ligation [13], we performed a similar experiment with human monocytic leukemia U937 cells that were made susceptible to Stx by transducing the CD77 synthase gene (further described later). Biotinyl-VAD-fmk bound to caspase 9 in Stx-treated cells, whereas this compound bound to caspases 8 and 10 in the TNFα-treated U937 cells (Fig. 2B). These data indicate that caspase 9 was initially activated in Stx-treated cells, which contrasted with caspase 8/10 activation by death receptor ligation.

To further confirm the caspase 9 as the initiator caspase in Stx-treated cells, we examined the formation of the apoptosome. In the mitochondrial pathway of apoptosis, cytochrome c released from mitochondria recruits Apaf1 and caspase 9 to form a huge complex called the apoptosome, which in turn cleaves and activates downstream effector caspases [30]. Four hours after Stx treatment when caspase 9 is not fully activated, a significant amount of Apaf1 was co-precipitated with caspase 9 (Fig. 2C). Similarly, Apaf1 was co-precipitated with caspase 9 in etoposide-treated THP1 cells. These results suggest that caspase 9 is the primary upstream caspase that initiates apoptosis in Stx-treated cells.

3.2. CD77 is required for induction of apoptosis by Stx

Stx binds to the cell surface CD77 to show its cytotoxic effects [10]. Since Stx did not induce apoptosis in most human cell lines including U937 cells (Table 1, Fig. 3A), we reasoned these cell lines do not undergo apoptosis because they lack CD77. To examine whether Stx-induced apoptosis is mediated through CD77, we transduced the CD77 synthase gene [23,24] into U937 cells and established several clones constitutively expressing CD77 synthase (Fig. 3B). Fig. 3C shows that all the clones expressing CD77 synthase exposed CD77 on the cell surface. We next examined the induction of apoptosis by Stx in the CD77 synthase transfectants. Stx treatment effectively induced apoptosis in all the clones (Fig. 3D), while it did not induce apoptosis in the parental U937 cells. In line with this, Stx-treatment induced the activation of caspases in the transfectants (Fig. 3E) and z-VAD-fmk inhibited activation of the caspase (Fig. 3F), as observed in THP1 cells (Fig. 5B). Ectopically expression of CD77 synthase does not seem to affect other signaling pathways of U937 cells, because CD77 synthase transfectants activate caspase cascade in response to death ligand ligation (Fig. 2B, TNF) and etoposide (data not shown) and proliferate as well as parent U937 cells. These results indicate that CD77 is required for Stx-induced caspase activation and apoptosis.

3.3. A-subunit of Stx plays an important role in the induction of apoptosis

To understand the role of the A-subunit in Stx-induced apoptosis, we treated THP1 cells with an A-subunit mutant

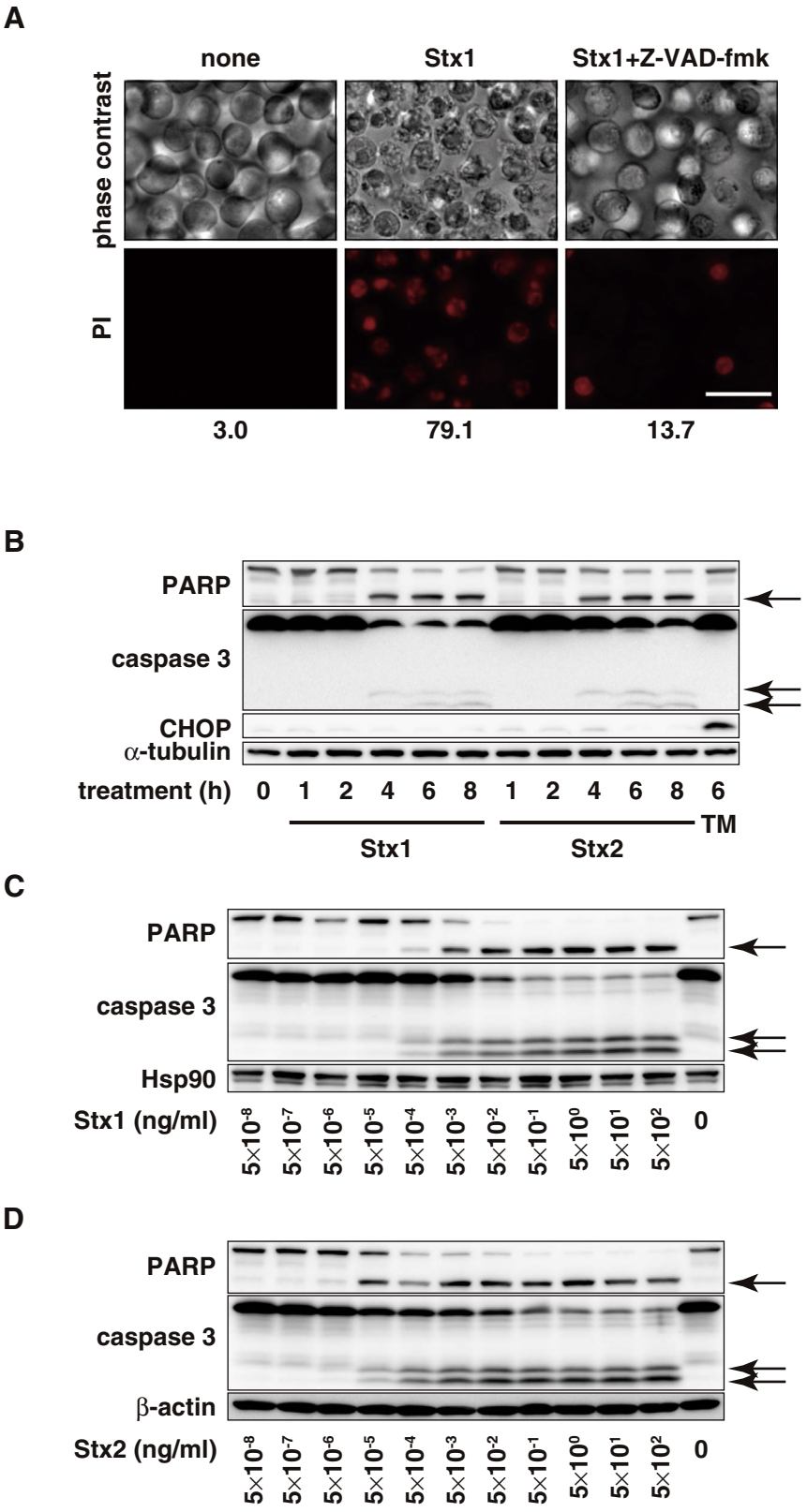

Fig. 1. Stx induces apoptosis. (A) THP1 cells were treated with or without 50 μM Z-VAD-fmk. After 30 min, the cells were treated with 100 pg/ml Stx1 for 24 h then the cells were stained with PI. PI-positive cells were observed under the fluorescent microscope and counted with a flow cytometer. The percentage of PI-positive cells is indicated at the bottom. Bar: 25 μm. (B) THP1 cells were treated with 1 ng/ml Stx1, Stx2 or 2 μg/ml tunicamycin (TM) for the indicated periods. Whole cell lysates were analyzed by Western blotting with the indicated antibodies. The arrows show cleaved caspase 3 and PARP. (C and D) THP1 cells were treated with the indicated doses of Stx1 (C) or Stx2 (D) for 6 h. Whole cell lysates were analyzed by Western blotting with the indicated antibodies. The arrows show cleaved caspase 3 and PARP.

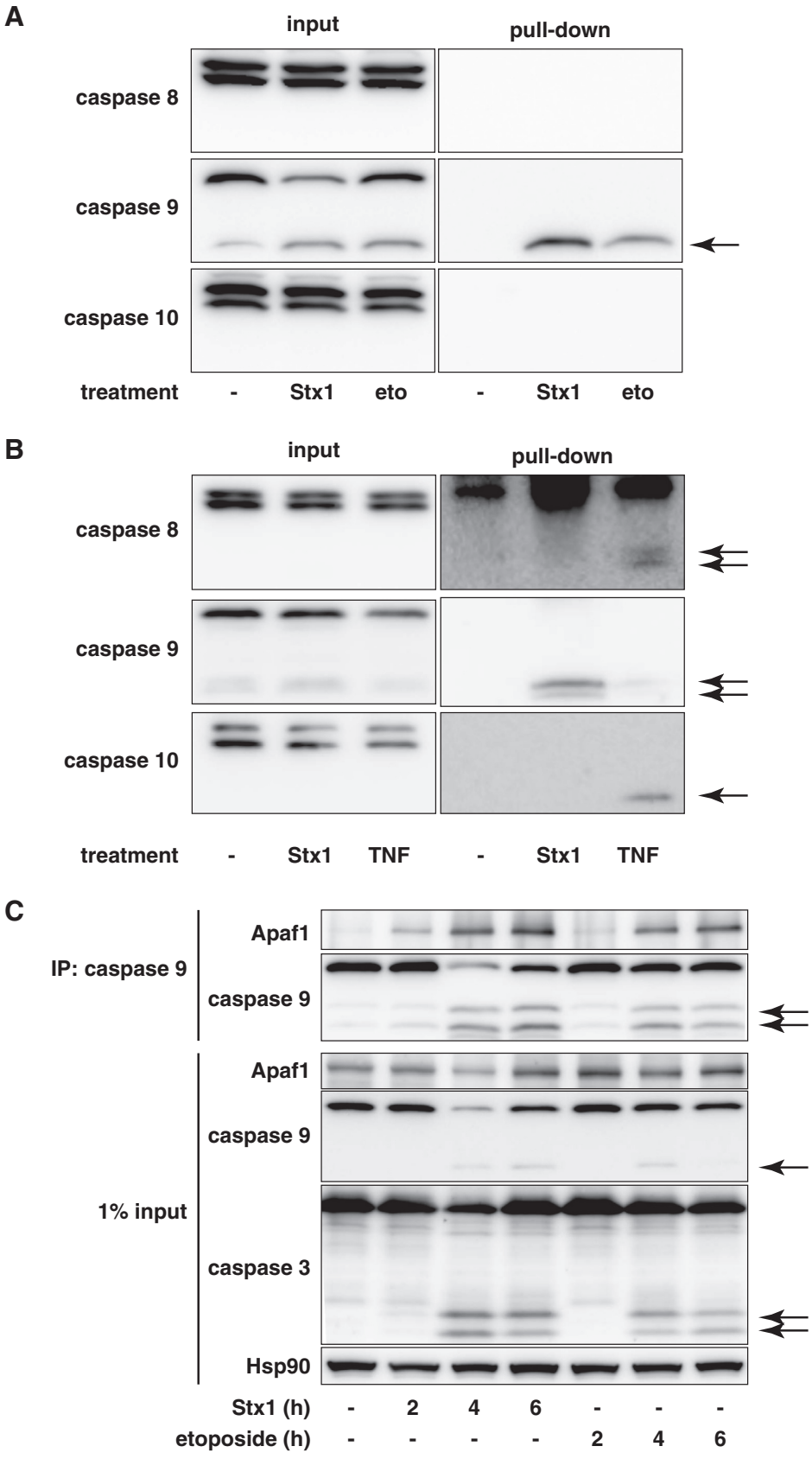

Fig. 2. Caspase 9 is initially activated in Stx-treated cells. (A and B) THP1 cells (A) or U937 cells that had been transfected with the CD77 synthase gene (clone 2) (B) were pre-treated with 50 μM biotinyl-VAD-fmk for 1 h, then the cells were treated with 1 ng/ml Stx1 for 4 h, 20 μg/ml etoposide for 4 h, or 1 μg/ml cycloheximide + 100 ng/ml TNF for 2 h. Cell lysates were analyzed by a pull-down assay with streptavidin-agarose. The precipitates and cell lysates were analyzed with the indicated antibodies. The arrows show the precipitated active caspase fragments. (C) THP1 cells were treated with 10 ng/ml Stx1 or 20 μg/ml etoposide for the indicated periods. Cell lysates were analyzed by immunoprecipitation (IP) with an anti-caspase 9 antibody. The precipitates and cell lysates were analyzed with the indicated antibodies. The arrows show cleaved caspases.

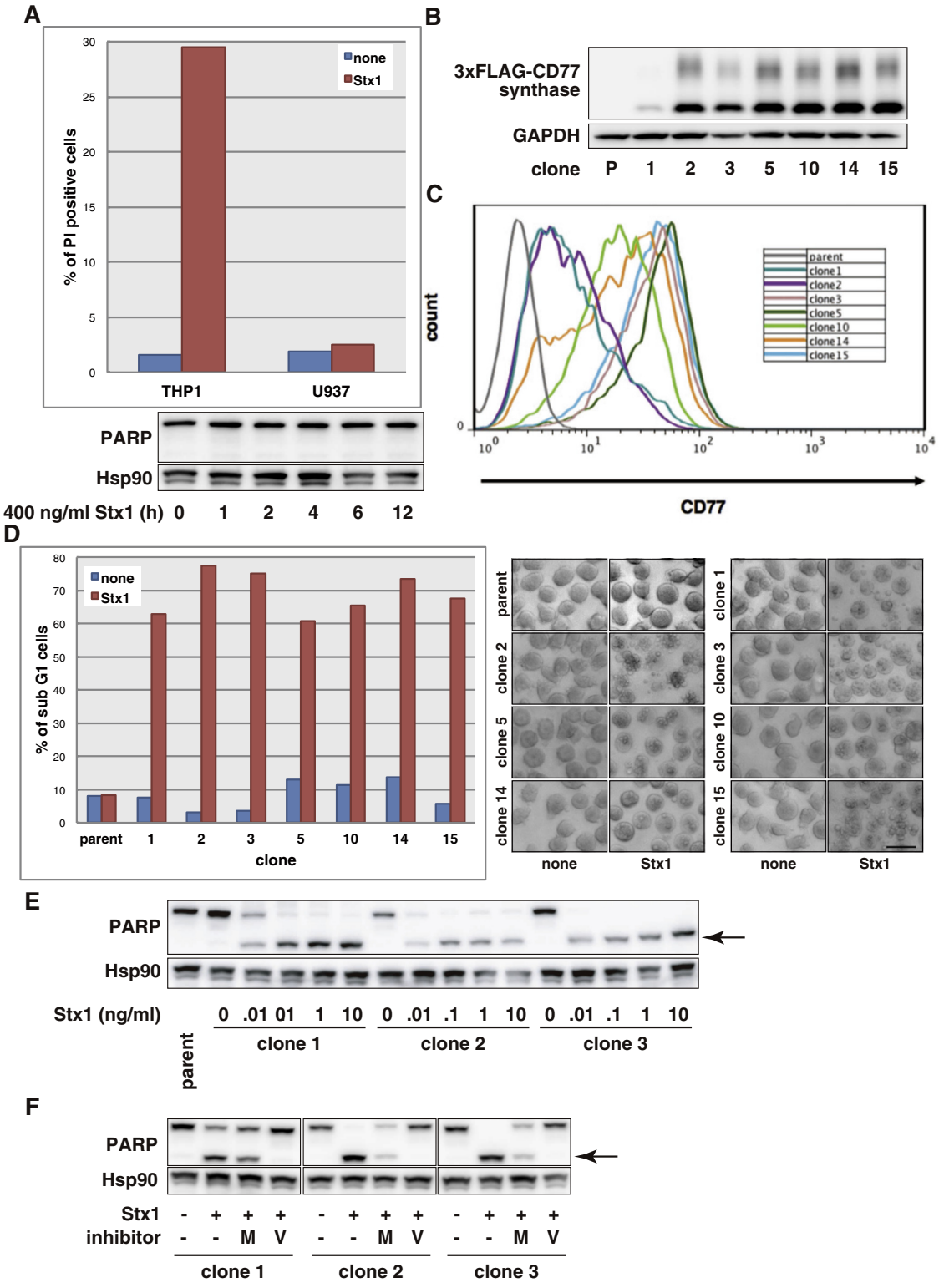

Fig. 3. Stx induces apoptosis in a CD77-dependent manner. (A) Upper panel: THP1 cells (1 ng/ml) and U937 cells (500 ng/ml) were treated with Stx1 for 10 h then the cells were stained with PI. PI-positive cells were counted with a flow cytometer. Lower panel: U937 cells were treated with 400 ng/ml Stx1 for the indicated periods. Whole cell lysate was analyzed by Western blotting with the indicated antibodies. (B) U937 cell clones constitutively expressing 3 × FLAG-CD77 synthase were obtained as described in Section 2.4. The total cell lysate of parent U937 cells (P) and the transfectant clones was analyzed by Western blotting with the indicated antibodies. (C) Cell surface CD77 was stained with FITC-conjugated anti-CD77 mAb. Expression levels of CD77 on CD77 synthase-transfected U937 clones were measured with a flow cytometer. (D) CD77 synthase-transfected U937 clones were treated with 1 ng/ml Stx1 for 6 h, then the cells were stained with PI. Sub-G1 cells were counted with a flow cytometer. The cell image was taken with a phase contrast microscope. Bar: 25 μm. (E) CD77 synthase-transfected U937 clones were treated with the indicated doses of Stx1 for 4 h. Whole cell lysates were analyzed by Western blotting with the indicated antibodies. The arrow shows cleaved PARP. (F) CD77 synthase-transfected U937 cell clones were treated with 10 μM MG132 (M) or 50 μM Z-VAD-fmk (V). After 30 min, the cells were treated with 1 ng/ml Stx1 for 6 h. Whole cell lysates were analyzed by Western blotting with the indicated antibodies. The arrow shows cleaved PARP.

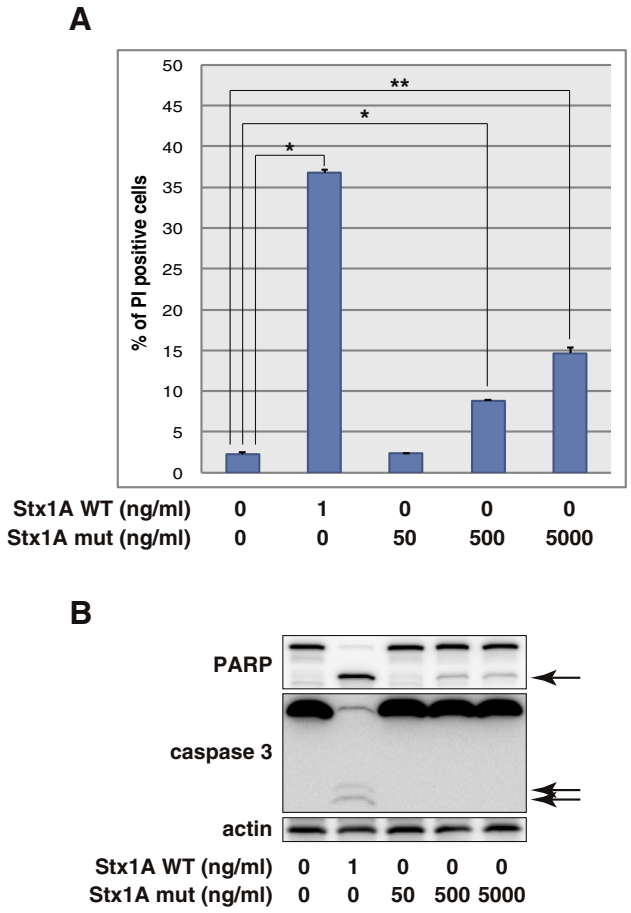

Fig. 4. Stx1 A-subunit mutant does not induce apoptosis. THP1 cells were treated with the indicated doses of wild-type Stx1 (Stx1A WT) and Stx1 A-subunit mutant (Stx1A mut) for 10 h, then the cells were stained with PI. PI-positive cells were counted with a flow cytometer (A). Values are the means ± standard deviation of three independent cultures. Parallel samples were analyzed by Western blotting with the indicated antibodies (B). The arrows show cleaved PARP and caspase 3. Asterisks represent a statistically significant difference from the values at untreated control cells ($^{*}p < 0.0005$, $^{**}p < 0.005$, *t*-test).

(E167Q/R170L) of Stx1 that possesses impaired activity to deadenylate 28S rRNA and inhibit protein synthesis [22]. As shown in Fig. 4, the Stx1A mutant had much lower activity than wild-type Stx1 to induce apoptosis. Even a 5000-fold excess amount of the Stx1A mutant induced minimal apoptosis (Fig. 4A) with negligible caspase activation (Fig. 4B). These data indicate that the functional A-subunit is required for the induction of caspase activation and apoptosis.

3.4. Proteasome activity is required for induction of apoptosis

To further explore the mechanism underlying Stx-induced apoptosis, we next analyzed apoptosis inhibitory proteins in response to Stx treatment. When THP1 cells were treated with Stx1, the expression of apoptosis inhibitory proteins Apollon, XIAP, c-IAP1, FLIP and Mcl-1 decreased prior to or along with caspase 3 activation. In contrast, the expression of Bcl-2 and Bcl-x were unchanged (Fig. 5A). Co-treatment with zVAD-fmk suppressed the Stx-induced reduction of Apollon and XIAP, but not c-IAP1, FLIP and Mcl-1, indicating that the reduction of c-IAP1, FLIP and Mcl-1 precedes caspase activation while Apollon and XIAP were cleaved by caspases as a result of apoptosis progression (Fig. 5B). Interestingly, the reduction of the apoptosis inhibitory proteins and caspase activation (Fig. 5B), and the extent of apoptosis (Fig. 5C) were all suppressed by a proteasome inhibitor MG132. We also observed that MG132 inhibited activation of caspases in CD77 synthase transfectant U937 cell clones (Fig. 3F). Similar results were obtained with a clinically approved proteasome inhibitor bortezomib (Fig. 5D). These results suggest that, upon Stx treatment, the levels of particular apoptosis inhibitory proteins decreased owing to proteasomal degradation followed by caspase activation and apoptosis progression.

3.5. Bortezomib extends the survival of mice challenged by Stx

Since bortezomib suppresses Stx-induced apoptosis *in vitro*, we then examined whether it can suppress the toxicity of Stx *in vivo* (Fig. 6A). We have established previously the model of Stx2 intoxication by intravenous injection [31]. In this model, administration of Stx2 resulted in the death of >90% of the mice within 3 days (Fig. 6B, red). The survival time was slightly extended by a single dose of 2 mg/kg of bortezomib 6 h prior to the Stx2 challenge (green). The extension of the survival was more markedly observed when mice were administered 1 mg/kg bortezomib twice (blue). The median of survival time, when half of the mice in each group died, was shifted from 68 h in the control group (red) to 76.5 h in the BRZ2 + Stx2 group (green) and 86 h in the BRZ1 × 2 + Stx2 group (blue). These results imply that inhibition of the proteasome may be beneficial to treat patients affected by Stx intoxication.

4. Discussion

In this study, the mechanism of how Stx induces apoptosis in THP1 cells and CD77 synthase-transduced U937 cells was investigated. The results demonstrated that CD77 and the *N*-glycosidase activity of the A-subunit are required for the Stx-induced apoptosis (Figs. 3 and 4). These observations are consistent with the mechanism by which Stx inhibits protein synthesis. Therefore, inhibition of protein synthesis is likely to play an essential role in Stx-induced apoptosis. As a result of protein synthesis inhibition, the levels of short-lived apoptosis inhibitory proteins rapidly decrease via proteasomal degradation (Fig. 5), which is followed by activation of an initiator caspase, caspase 9 (Fig. 2), and an executioner caspase, caspase 3, to execute apoptosis (Fig. 1).

The reduction of apoptosis inhibitory proteins by Stx is crucial but likely insufficient to induce apoptosis, since cycloheximide, an inhibitor of protein synthesis, also reduces the apoptosis inhibitory proteins but cannot induce apoptosis in THP1 cells (Hattori and Naito, unpublished data). In many cells, cycloheximide sensitizes cells to apoptosis induced by death receptor ligation, which is explained by the reduction of short-lived apoptosis inhibitory proteins [32–35]. In these cells, caspase activation is remarkably enhanced by various apoptosis stimuli. Therefore, we postulate that the ability of Stx to inhibit protein synthesis sensitizes the cells to apoptosis by reducing apoptosis inhibitory proteins, and Stx simultaneously triggers caspase activation by an additional mechanism to induce apoptosis. Currently, the triggering mechanism of caspase activation by Stx is not understood, but the *N*-glycosidase activity of the A-subunit is also required for triggering. Possibly, the deadenylated 28S ribosome is recognized by a cellular damage sensor, which mediates apoptosis signaling to mitochondria.

We identified caspase 9 as a primary upstream caspase that initiates apoptosis in Stx-treated cells. However, there are some reports that suggest a role of caspase 8 as an initiator caspase in Stx-treated cells [15–18]. In some of these studies, they observed ER stress responses including CHOP expression, which induces the expression of TRAIL and DR5 resulting in activation of caspase

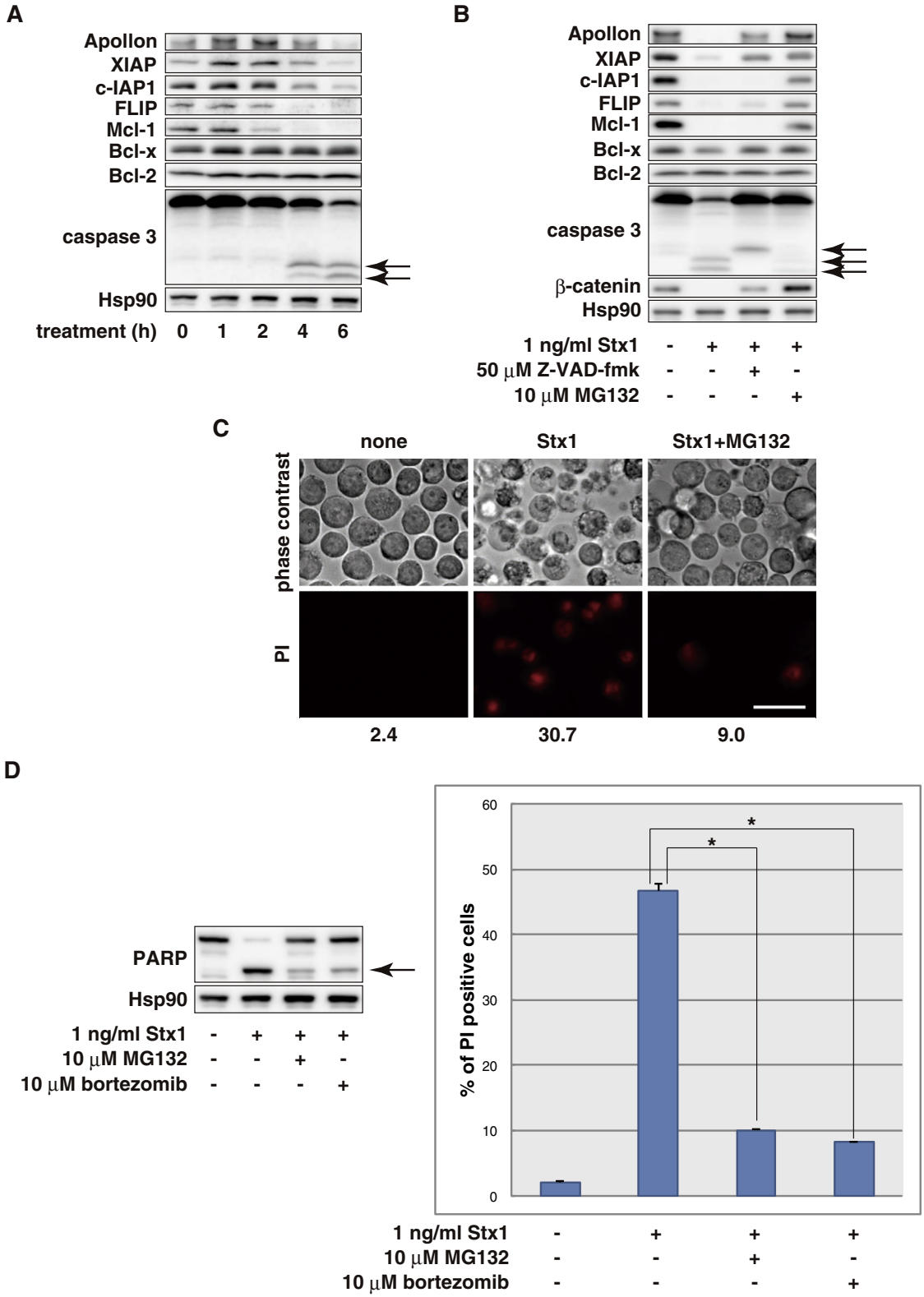

Fig. 5. Proteasome inhibitors prevent Stx-induced apoptosis. (A) THP1 cells were treated with 1 ng/ml Stx1 for the indicated periods. The whole cell lysate was analyzed by Western blotting with the indicated antibodies. The arrows show cleaved caspase 3. (B) THP1 cells were treated with 1 ng/ml Stx1 for 6 h in the absence or presence of 10 μM MG132 or 50 μM Z-VAD-fmk. The whole cell lysate was analyzed by Western blotting with the indicated antibodies. The arrows show cleaved caspase 3. (C) THP1 cells were treated with 100 pg/ml Stx1 in the absence or presence of 10 μM MG132 for 10 h then the cells were stained with PI. PI-positive cells were observed with the fluorescent microscope and counted with a flow cytometer. The percentage of PI-positive cells is indicated at the bottom. Treatment with 10 μM MG132 alone resulted in modest cell death (9.6%). Bar: 25 μm. (D) THP1 cells were treated with 1 ng/ml Stx1 with or without 10 μM MG132 or 10 μM bortezomib for 10 h, then the cells were stained with PI. PI-positive cells were counted with a flow cytometer. Values are the means ± standard deviation of three independent cultures. Parallel samples were analyzed by Western blotting with the indicated antibodies. Treatment with 10 μM MG132 and 10 μM bortezomib alone induced modest cell death (14.92 ± 0.37% and 17.42 ± 1.00%, respectively). The arrows show cleaved PARP. Asterisks represent a statistically significant difference from the values at Stx1 alone ($p < 0.0005$, t-test).

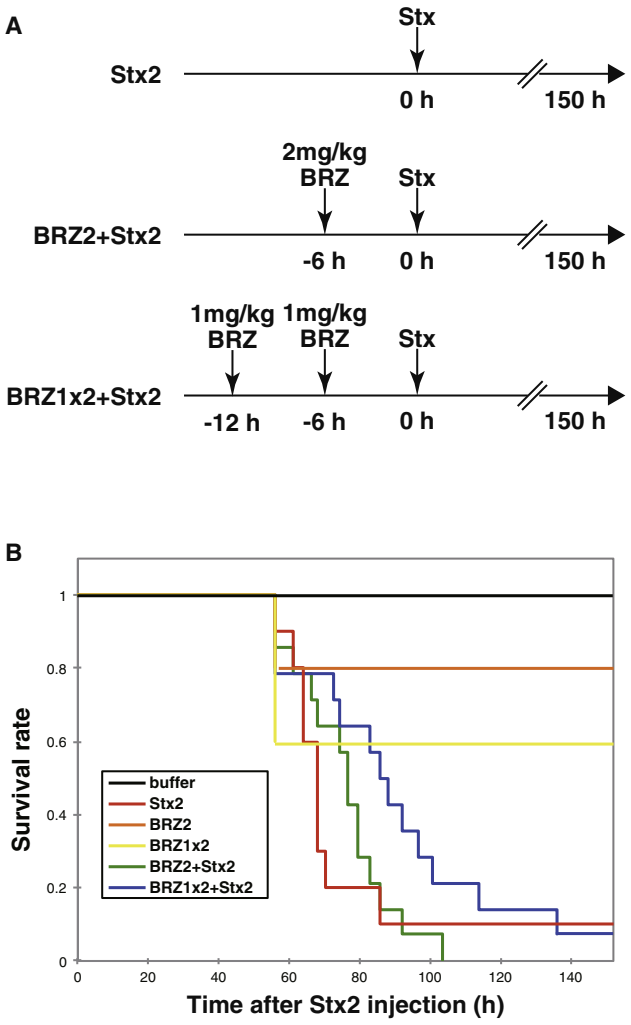

Fig. 6. Bortezomib prolongs survival of mice challenged by a lethal dose of Stx2. (A) Experimental procedure for administration of bortezomib (BRZ) and Stx2. (B) Survival of Stx-intoxicated mice. Mice were treated with vehicle (buffer, $n = 4$) or various doses of bortezomib. 6 h after the final bortezomib administration, the animals were challenged with a lethal dose of Stx2 (3 ng/20 g body weight) or vehicle. Stx2: mice were treated with Stx2 only ($n = 10$). BRZ2: mice were treated with 2 mg/kg bortezomib ($n = 5$). BRZ1 × 2: mice were treated with 1 mg/kg bortezomib for 6 h then the animals were treated with 1 mg/kg bortezomib again ($n = 5$). BRZ2 + Stx2: mice were treated with 2 mg/kg bortezomib prior to Stx2 challenge ($n = 14$). BRZ1 × 2 + Stx2: mice were treated with 1 mg/kg bortezomib twice prior to Stx2 challenge ($n = 14$). Data represent the survival rate of each group.

8 [15,16]. In our experimental conditions, however, CHOP was not induced and caspase 8 was not activated in the cells destined to undergo apoptosis (Figs. 1B, 2A and B). Inhibition of protein synthesis by cycloheximide did not affect Stx-induced apoptosis (Hattori and Naito, unpublished data), which further supports that CHOP synthesis is not involved in the Stx-induced apoptosis in our system. It is unclear why different responses are observed in the same cell line, but the doses of Stx are much higher in previous reports than our experiments, which may explain the differences in the cellular responses.

The short-lived apoptosis inhibitory proteins are degraded by the proteasome [32–36] and the inhibition of protein synthesis by Stx results in the reduction of those proteins (Fig. 5A). When cells were co-treated with proteasome inhibitors and Stx, the levels of apoptosis inhibitory proteins were maintained and the progression of apoptosis was suppressed (Fig. 5B–D). Our results are consistent with previous study which demonstrated that Stx reduced an apoptosis inhibitory protein Mcl-1 but not Bcl-2 and Bcl-x in a proteasome activity dependent manner and that inhibition of proteasome activity protected against caspase activation by Stx in endothelial cells [37]. Intriguingly, bortezomib [19] suppressed Stx-induced apoptosis *in vitro* (Fig. 5D) and extended the survival of mice challenged by Stx (Fig. 6). To our regret, the effective doses of bortezomib were quite high, which killed a considerable number of mice even when bortezomib was administrated alone, and most of the Stx-administered mice eventually died. However, our results suggest that suppression of apoptosis could be beneficial for patients affected by Stx intoxication and the inhibition of the proteasome could be a novel strategy to treat patients infected with STEC.

Conflict of interest

All authors declare no conflict of interest.

Acknowledgements

The authors thank Drs. Keiichiro Okuhira and Norihito Shibata for helpful discussions, and Mariko Seki and Toshio Sato for technical assistance.

This study was supported by Grants-in Aid for Scientific Research from the Ministry of Education, Culture, Sports, Science, and Technology, and by Health and Labor Sciences Research Grants, Japan.

KN and MN conceived and supervised the study; THat, MWT, KN and MN designed experiments; THat, MWT and NO performed experiments; THam and KF provided tools and reagents; THat and MWT analyzed data; THat, MWT, NK and MN interpreted the data; THat and MN wrote the manuscript; THat, KF, KN and MN made manuscript revisions.

References

[1] Karmali, M.A., Steele, B.T., Petric, M. and Lim, C. (1983) Sporadic cases of haemolytic-uraemic syndrome associated with faecal cytotoxin and cytotoxin-producing *Escherichia coli* in stools. Lancet 1, 619–620.
[2] O'Brien, A.D. and Holmes, R.K. (1987) Shiga and Shiga-like toxins. Microbiol. Rev. 51, 206–220.
[3] Paton, J.C. and Paton, A.W. (1998) Pathogenesis and diagnosis of Shiga toxin-producing *Escherichia coli* infections. Clin. Microbiol. Rev. 11, 450–479.
[4] Riley, L.W. et al. (1983) Hemorrhagic colitis associated with a rare *Escherichia coli* serotype. N. Engl. J. Med. 308, 681–685.
[5] Scheutz, F. et al. (2012) Multicenter evaluation of a sequence-based protocol for subtyping Shiga toxins and standardizing Stx nomenclature. J. Clin. Microbiol. 50, 2951–2963.
[6] Melton-Celsa, A.R. and O'Brien, A.D. (1998) Structure, biology, and relative toxicity of Shiga toxin family members for cells and animals in: *Escherichia coli* O157:H7 and Other Shiga Toxin-producing *E. coli* Strains (Kaper, J.B. and O'Brien, A.D., Eds.), pp. 121–128, American Society for Microbiology, Washington, DC.
[7] Karmali, M.A., Petric, M., Lim, C., Fleming, P.C., Arbus, G.S. and Lior, H. (1985) The association between idiopathic hemolytic uremic syndrome and infection by verotoxin-producing *Escherichia coli*. J. Infect. Dis. 151, 775–782.
[8] Endo, Y., Tsurugi, K., Yutsudo, T., Takeda, Y., Ogasawara, T. and Igarashi, K. (1988) Site of action of a Vero toxin (VT2) from *Escherichia coli* O157:H7 and of Shiga toxin on eukaryotic ribosomes. RNA N-glycosidase activity of the toxins. Eur. J. Biochem. 171, 45–50.
[9] Saxena, S.K., O'Brien, A.D. and Ackerman, E.J. (1989) Shiga toxin, Shiga-like toxin II variant, and ricin are all single-site RNA *N*-glycosidases of 28 S RNA when microinjected into *Xenopus* oocytes. J. Biol. Chem. 264, 596–601.
[10] Johannes, L. and Romer, W. (2010) Shiga toxins – from cell biology to biomedical applications. Nat. Rev. Microbiol. 8, 105–116.
[11] Ching, J.C., Jones, N.L., Ceponis, P.J., Karmali, M.A. and Sherman, P.M. (2002) *Escherichia coli* shiga-like toxins induce apoptosis and cleavage of poly(ADP-ribose) polymerase via in vitro activation of caspases. Infect. Immun. 70, 4669–4677.
[12] Kiyokawa, N. et al. (2001) Activation of the caspase cascade during Stx1-induced apoptosis in Burkitt's lymphoma cells. J. Cell Biochem. 81, 128–142.
[13] Lee, S.Y., Cherla, R.P., Caliskan, I. and Tesh, V.L. (2005) Shiga toxin 1 induces apoptosis in the human myelogenous leukemia cell line THP-1 by a caspase-8-dependent, tumor necrosis factor receptor-independent mechanism. Infect. Immun. 73, 5115–5126.

[14] Tetaud, C. et al. (2003) Two distinct Gb3/CD77 signaling pathways leading to apoptosis are triggered by anti-Gb3/CD77 mAb and verotoxin-1. J. Biol. Chem. 278, 45200–45208.
[15] Lee, M.S., Cherla, R.P., Leyva-Illades, D. and Tesh, V.L. (2009) Bcl-2 regulates the onset of shiga toxin 1-induced apoptosis in THP-1 cells. Infect. Immun. 77, 5233–5244.
[16] Lee, S.Y., Lee, M.S., Cherla, R.P. and Tesh, V.L. (2008) Shiga toxin 1 induces apoptosis through the endoplasmic reticulum stress response in human monocytic cells. Cell Microbiol. 10, 770–780.
[17] Garibal, J., Hollville, E., Renouf, B., Tetaud, C. and Wiels, J. (2010) Caspase-8-mediated cleavage of Bid and protein phosphatase 2A-mediated activation of Bax are necessary for Verotoxin-1-induced apoptosis in Burkitt's lymphoma cells. Cell Signal. 22, 467–475.
[18] Fujii, J. et al. (2003) Rapid apoptosis induced by Shiga toxin in HeLa cells. Infect. Immun. 71, 2724–2735.
[19] Adams, J. and Kauffman, M. (2004) Development of the proteasome inhibitor Velcade (Bortezomib). Cancer Invest. 22, 304–311.
[20] Hao, Y. et al. (2004) Apollon ubiquitinates SMAC and caspase-9, and has an essential cytoprotection function. Nat. Cell Biol. 6, 849–860.
[21] Nishikawa, K. et al. (2005) Identification of the optimal structure required for a Shiga toxin neutralizer with oriented carbohydrates to function in the circulation. J. Infect. Dis. 191, 2097–2105.
[22] Ohmura, M., Yamasaki, S., Kurazono, H., Kashiwagi, K., Igarashi, K. and Takeda, Y. (1993) Characterization of non-toxic mutant toxins of Vero toxin 1 that were constructed by replacing amino acids in the A subunit. Microb. Pathog. 15, 169–176.
[23] Kojima, Y. et al. (2000) Molecular cloning of globotriaosylceramide/CD77 synthase, a glycosyltransferase that initiates the synthesis of globo series glycosphingolipids. J. Biol. Chem. 275, 15152–15156.
[24] Okuda, T. et al. (2006) Targeted disruption of Gb3/CD77 synthase gene resulted in the complete deletion of globo-series glycosphingolipids and loss of sensitivity to verotoxins. J. Biol. Chem. 281, 10230–10235.
[25] Tu, S., McStay, G.P., Boucher, L.M., Mak, T., Beere, H.M. and Green, D.R. (2006) In situ trapping of activated initiator caspases reveals a role for caspase-2 in heat shock-induced apoptosis. Nat. Cell Biol. 8, 72–77.
[26] Hattori, T., Isobe, T., Abe, K., Kikuchi, H., Kitagawa, K., Oda, T., Uchida, C. and Kitagawa, M. (2007) Pirh2 promotes ubiquitin-dependent degradation of the cyclin-dependent kinase inhibitor p27Kip1. Cancer Res. 67, 10789–10795.
[27] Tesh, V.L. (2012) Activation of cell stress response pathways by Shiga toxins. Cell Microbiol. 14, 1–9.
[28] Ron, D. and Walter, P. (2007) Signal integration in the endoplasmic reticulum unfolded protein response. Nat. Rev. Mol. Cell Biol. 8, 519–529.
[29] Takeda, Y., Kurazono, H. and Yamasaki, S. (1993) Vero toxins (Shiga-like toxins) produced by enterohemorrhagic *Escherichia coli* (verocytotoxin-producing *E. coli*). Microbiol. Immunol. 37, 591–599.
[30] Li, P., Nijhawan, D., Budihardjo, I., Srinivasula, S.M., Ahmad, M., Alnemri, E.S. and Wang, X. (1997) Cytochrome c and dATP-dependent formation of Apaf-1/caspase-9 complex initiates an apoptotic protease cascade. Cell 91, 479–489.
[31] Nishikawa, K. et al. (2002) A therapeutic agent with oriented carbohydrates for treatment of infections by Shiga toxin-producing *Escherichia coli* O157:H7. Proc. Natl. Acad. Sci. U.S.A. 99, 7669–7674.
[32] Chang, L., Kamata, H., Solinas, G., Luo, J.L., Maeda, S., Venuprasad, K., Liu, Y.C. and Karin, M. (2006) The E3 ubiquitin ligase itch couples JNK activation to TNFalpha-induced cell death by inducing c-FLIP(L) turnover. Cell 124, 601–613.
[33] Kreuz, S., Siegmund, D., Scheurich, P. and Wajant, H. (2001) NF-kappaB inducers upregulate cFLIP, a cycloheximide-sensitive inhibitor of death receptor signaling. Mol. Cell Biol. 21, 3964–3973.
[34] Micheau, O., Lens, S., Gaide, O., Alevizopoulos, K. and Tschopp, J. (2001) NF-kappaB signals induce the expression of c-FLIP. Mol. Cell Biol. 21, 5299–5305.
[35] Wang, L., Du, F. and Wang, X. (2008) TNF-alpha induces two distinct caspase-8 activation pathways. Cell 133, 693–703.
[36] Sekine, K. et al. (2008) Small molecules destabilize cIAP1 by activating auto-ubiquitylation. J. Biol. Chem. 283, 8961–8968.
[37] Erwert, R.D., Eiting, K.T., Tupper, J.C., Winn, R.K., Harlan, J.M. and Bannerman, D.D. (2003) Shiga toxin induces decreased expression of the anti-apoptotic protein Mcl-1 concomitant with the onset of endothelial apoptosis. Microb. Pathog. 35, 87–93.